

Spatio-Temporal Scene Graphs for Video Dialog

Shijie Geng¹ Peng Gao² Chiori Hori³ Jonathan Le Roux³ Anoop Cherian³

¹Rutgers University, Piscataway, NJ ²Chinese University of Hong Kong
³Mitsubishi Electric Research Labs (MERL), Cambridge, MA

Abstract. The Audio-Visual Scene-aware Dialog (AVSD) task requires an agent to indulge in a natural conversation with a human about a given video. Specifically, apart from the video frames, the agent receives the audio, brief captions, and a dialog history, and the task is to produce the correct answer to a question about the video. Due to the diversity in the type of inputs, this task poses a very challenging multimodal reasoning problem. Current approaches to AVSD either use global video-level features or those from a few sampled frames, and thus lack the ability to explicitly capture relevant visual regions or their interactions for answer generation. To this end, we propose a novel *spatio-temporal scene graph representation* (STSGR) modeling fine-grained information flows within videos. Specifically, on an input video sequence, STSGR (i) creates a two-stream visual and semantic scene graph on every frame, (ii) conducts intra-graph reasoning using node and edge convolutions generating visual memories, and (iii) applies inter-graph aggregation to capture their temporal evolutions. These visual memories are then combined with other modalities and the question embeddings using a novel semantics-controlled multi-head shuffled transformer, which then produces the answer recursively. Our entire pipeline is trained end-to-end. We present experiments on the AVSD dataset and demonstrate state-of-the-art results. A human evaluation on the quality of our generated answers shows 12% relative improvement against prior methods.

Keywords: Scene graphs, video dialog, graph convolution networks

1 Introduction

The success of deep learning in producing effective solutions to several fundamental problems in computer vision, natural language processing, and audio/speech understanding has served as an impetus to explore more complex multimodal problems at the intersections of these domains, attracting wide interest recently [71]. A few notable such multimodal problems include (i) visual question answering (VQA) [3,60], the goal of which is to build an agent that can generate correct answers to free-form questions about visual content, (ii) audio/visual captioning [24,52,59,14], in which the agent needs to generate a natural language sentence describing the audio/visual content, (iii) visual dialog [9], in which the agent needs to engage in a natural conversation with a human about a static image, and (iv) audio-visual scene-aware dialog (AVSD) [1,23] –

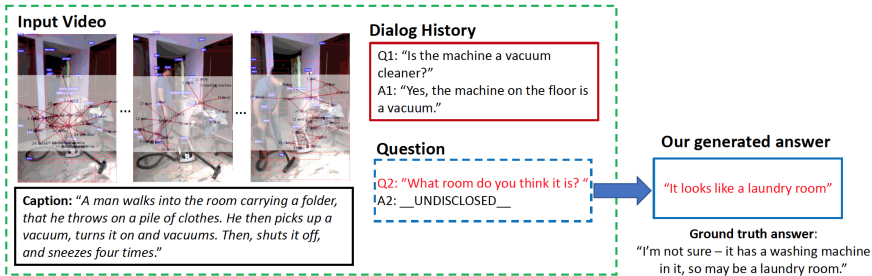


Fig. 1. A result from our STSGR model illustrating the AVSD task. It takes as input a video clip, its caption, dialog history, and a question, and the task is to generate the answer. As our goal in this paper is on visual representation learning, we do not use the audio stream. We also show the scene graphs for each frame generated by our method.

that generalizes (i), (ii), and (iii) – in which the agent needs to produce a natural answer to a question about a given audio-visual clip, in a conversation setting. As is clear, the ASVD task emulates a real-world human-machine conversation setting,¹ that is potentially useful in a variety of practical scenarios, such as building virtual assistants [12] or controlling human-robot interactions [47].

The generality of the AVSD task, however, poses a challenging multimodal representation learning and reasoning problem. Specifically, some of the input modalities to this task may offer complementary information (such as video and audio), while a few others may be independent (audio and captions), or even conflict with each other, e.g., the provided text (captions/dialogs) may include details from human experience that are absent in the video (“I think...”), or may include abstract responses (“happy”, “bored”, etc.) that may be subjective. Thus, the fundamental question this task highlights is how to effectively represent these modalities such that the inference is efficient and effective. Previous approaches to this problem typically use holistic video features produced by a generic 3D convolutional neural network [5], and either focused on extending attention models on these features to include additional modalities [1,23,44], or use powerful transformer networks [50] to produce effective multimodal embeddings [31]. These methods perhaps undermined the importance of fine-grained visual representations, as such 3D networks are usually trained for human action recognition tasks, and thus may not explicitly capture details of objects or their relationships within the video frames. Further, the convolution filters that are used in such networks usually operate on regular grids, thus failing to capture exclusive information regarding visual entities and their properties, as is shown for static images in [2,30].

In this paper, we present neural inference algorithms that hierarchically reduce the complexity of the AVSD task using the machinery of graph neural

¹ The AVSD dataset [1] does not include speech in its audio-stream. Nevertheless, text-based dialogs are very close to oral conversations now-a-days, thanks to the advancements in automatic speech recognition technologies.

networks. Specifically, we propose a novel spatio-temporal scene graph representation (STSGR) on the video in which each video frame is characterized using a scene graph [28]. The nodes of this graph correspond to visual features and their semantic labels from detections produced by a pre-trained object detector [2], while the graph edges capture the relations between the nodes as produced using a relationship detector [30]. As not all nodes and edges are relevant for our task, we use intra- and inter- graph pooling using neural message passing [51] to succinctly characterize graph components and their spatio-temporal evolution. Our STSGR results in visual memories which are embeddings of each video frame, which are subsequently fused with other modalities and the input question using a semantics-controlled multimodal transformer, thereby generating the answer sentence, one word at a time. In comparison to a standard transformer [50] that uses a fixed concatenation of features from all heads to generate the embeddings, we propose to shuffle the heads; our experiments show that this step improves generalization of the embeddings produced.

To empirically evaluate STSGR, we present elaborate experiments on AVSD datasets available as part of the 7th and 8th Dialog System Technology Challenges (DSTC). Our results on the DSTC test sets reveal that using the proposed STSGR representation leads to significant improvements in the generated answers against state of the art methods on all the language metrics. Further, an independent human evaluation conducted by the organizers of the DSTC challenge shows that our generated answers are more than 12% better (relatively) than previous baselines in preference.

Before proceeding to exposit our method in detail, we summarize our key contributions below.

- We propose to represent videos as two spatio-temporal scene graphs capturing fine-grained visual cues and semantic structure respectively. It is the first attempt at applying such a representation for the video dialog task.
- Our STSGR involves graphs for every frame that are difficult to be used for inference. To this end, we propose to encode them hierarchically using intra-graph reasoning and inter-graph information aggregation, that benefit further higher-level reasoning through transformer structures [50]. We further propose semantically-controlled transformers using shuffled multi-heads for multimodal fusion, language modeling, and sequential answer generation.
- Extensive experiments and ablation studies on the AVSD answer generation task demonstrate that our approach is better at modeling the visual cues and outperforms several challenging recent baselines on this task.

2 Related Work

Our proposed framework has similarities with prior works on four different axes, namely (i) graph-based reasoning, (ii) multimodal attention, (iii) visual dialog methods, and (iv) video representation learning. Below, we explicitly review these methods and point out the key differences.

Scene Graphs: [28] combines objects detected in static images [2,43], their attributes [15], and object-object relationships [37] to form a directed graph that not only provides an explicit and interpretable representation of the image, but is also seen to be beneficial for higher-order reasoning tasks such as image captioning [36,62,63], and visual question answering [21,46,41]. While, we are not aware of any prior published work that generalizes scene graphs for video data, there have been efforts [53,22,26] at capturing spatio-temporal evolution of localized visual cues. In [54], Wang and Gupta propose a space-time graph reasoning framework for human action recognition. Similar to ours, they use object detections per video frame, and construct a spatio-temporal graph based on the affinities of the features from the detected objects. In contrast, our video dialog task is more complex and demands a scene representation that is more detailed, requiring a graph architecture that is very different from [54], involving several sub-modules of graph reasoning, graph pooling, and representation learning. In [27], Jang et al. propose a spatio-temporal reasoning framework for video question answering, however without using a graph structure for scene representation. In [49], a temporal conditional random field is proposed, but for the problem of visual relationship prediction. We also note that scene graph generation from static images has been an important research problem in recent times [7,13,39,61,66], advancements to which are complementary to our efforts in this paper.

Multimodal Fusion/Attention: As data from various modalities (text, audio, vision, etc.) have different properties, they may belong to disconnected subspaces, posing difficulties in joint inference. Bilinear fusion methods [4,16] have been explored towards inter-modality semantic alignment, however they often result in high-dimensional interaction tensors that can be computationally expensive during inference. There are also prior methods that propose interesting ways to fuse the modalities, such as predicting fully-connected layer weights [40], introducing scale normalization layers [11], and learning convolution kernels [19] by conditioning on the other modality. Attention-based fusion [24,25,23], in contrast, fuses the modalities hierarchically, thus leading to cheaper computations, while also demonstrating compelling performance. Self-attention and feature embeddings using transformer networks [50] have recently demonstrated very promising results in the language arena, and have been explored in multimodal settings [18] similar to ours, however on static images.

Multimodal Dialog: Visual dialog has been explored in various ways before. For example, de Vries et al. [10] introduced the “Guess What!” dataset and the associated two-player guessing game for visual dialogs, while Geman et al. [20] proposed dialogs as a visual Turing test; both methods only considered answers in a binary “Yes/No” setting. Free-form human-like answers were first considered in [9], which also proposed the VisDial dataset, however only dialogs on static images were considered, in contrast with the AVSD task [1] that we tackle in this paper. As alluded to above, a common difficulty in designing algorithms on multimodal data is in deriving effective attention mechanisms that can divulge information from disparate modalities. To tackle this challenge, Wu et

al. [56] proposed a sequential co-attention scheme in which the neural embeddings of various modalities are co-attended with visual embeddings in a specific order. Schwartz et al. [45] generalized the co-attention problem by treating the modalities as nodes of a graph, and aggregated nodes – representing factors – are obtained using neural message passing. We use a combination of these two approaches; specifically we use powerful transformer encoders [50] for embedding each modality, and attend on these embeddings sequentially to generate the answer. Further, in contrast to [45,56], that tackle an answer selection problem, we consider a free-form answer generation task in AVSD, in which the response is generated one word at a time. Yeh et al. [64] also proposed using transformers [50] for fusing audio-visual features on the AVSD task. A multi-step reasoning scheme is proposed in [17] using joint attention via an RNN for generating a multimodal representation. The Simple baseline [44] extends factor graphs [45] for the AVSD problem demonstrating promising results. A multimodal transformer for embedding various modalities and a query-aware attention is introduced in [31]. However, these works do not consider richer visual representations using scene graphs.

Temporal Representation Learning: Learning video representations is an important ingredient to any spatio-temporal reasoning task. As we alluded to above, prior methods for video dialog [1,23,33,58] capitalized on advancements in video-based action recognition frameworks, such as the C3D [48] and the inflated 3D [5] networks. However, as noted above, these frameworks use fixed (and regular) grids for feature generation, and thus lack the flexibility in reasoning over evolving spatio-temporal regions, which is crucial for tasks such as question answering. Spatio-temporal graph convolutional networks have been explored earlier, such as in Yu et al. [65] and related methods [57,70], however, these methods assume a given (and often fixed) graph structure. However, our scene graphs’ structure can change from frame to frame as decided by our detector modules, thus requiring significantly different inference schemes.

3 Spatio-Temporal Scene Graph Reasoning

Given a video sequence V , let C denote the associated human-generated video caption, and let (Q_i, A_i) represent the tuple of the text-based i -th question and its answer in the given human dialog about V (see Fig. 1). We will succinctly represent the dialog history by $H = \langle (Q_1, A_1), \dots, (Q_{l-1}, A_{l-1}) \rangle$. Further, let Q_l represent the pertinent question. The audio-visual scene-aware dialog (AVSD) task requires the generation of a correct human-like answer, denoted A_l , for the question Q_l .

Our proposed STSGR approach to solve this task is schematically illustrated in Fig. 2. It consists of four components: (1) a *scene graph construction module*, which extracts objects and relation proposals from the video using pretrained neural network models, building a scene graph for every (temporally-sampled) video frame, (2) an *intra-graph reasoning module*, which conducts node-level and edge-level graph reasoning and generates visual memory for each frame’s

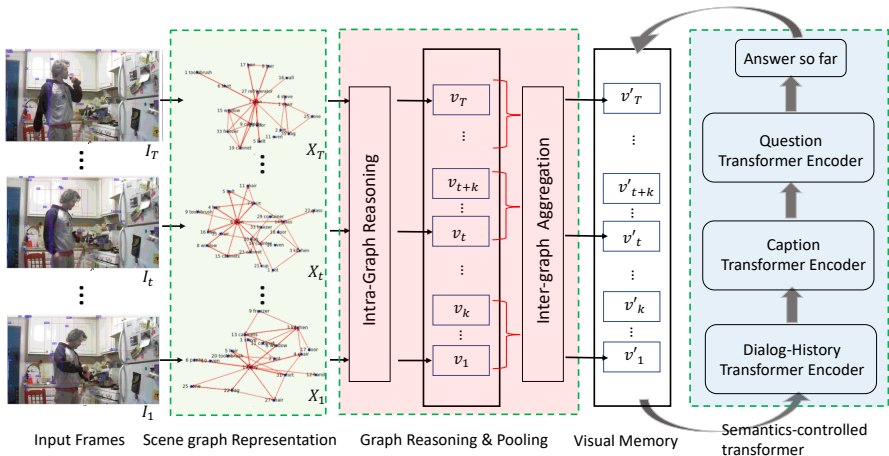


Fig. 2. A schematic illustration of our overall STSGR pipeline.

scene graph, (3) an *inter-graph information aggregation module*, which aggregates graph memories of contextual frames within a sliding window to update the graph memory of the center frame in that window, (4) a *semantics-controlled transformer reasoning module*, which performs multimodal reasoning and language modelling based on a semantic controller. In this module, we also use a newly-proposed shuffle-augmented co-attention to enable head interactions in order to boost performance. Below, we describe in detail each of these modules.

3.1 Scene Graph Representation of Video

Recent works [2,34,35] have demonstrated that adopting fine-grained bottom-up and top-down visual information significantly improves the performance of multimodal reasoning problems, especially on sentence generation tasks. Inspired by this observation, we propose to extract fine-grained information from sampled video frames. We first build a scene graph that consists of objects and their visual relationships, to represent individual frames. Naturally, each video can be represented as a sequence of such scene graphs. Our scene graph representation module can be decomposed into three parts: (a) object detection and extraction of visual and semantic features, (b) visual-relation proposal generation and object filtering, and (c) region of interest (ROI) recrop on union bounding boxes.

Object Detection: This module aims at detecting objects and extracting visual features and their semantics. Similar to Anderson et al. [2], we train a Faster R-CNN model [43] on the Visual Genome [30] using the MMDetection repository [6]. For some video frame I , this Faster-RCNN model produces

$$\mathcal{F}_I, \mathcal{B}_I, \mathcal{S}_I = \text{RCNN}(I), \quad (1)$$

where $\mathcal{F}_I \in \mathbb{R}^{N_o \times d_o}$ denotes the d_o -dimensional object features, $\mathcal{B}_I \in \mathbb{R}^{N_o \times 4}$ are the object bounding boxes, and \mathcal{S}_I is a list of semantic labels associated with each bounding box. In our trained model, we consider $N_o = 36$ detections with $d_o = 1024$ (from the ResNext-101 as backbone we use with multi-scale feature pyramid network) and use a semantic label vocabulary of size 1601.

Relation Proposal Generation: This module aims at recognizing the visual relations between the detected objects in a sampled frame and generating a fixed number N_r of relation proposals with the highest confidences. We use the approach in Zhang et al. [67] to detect visual relations in each frame. Specifically, we train a relation model on the VG200 dataset [30], which contains 150 objects and 50 predicates, and apply this learned model on sampled frames from a given video. The output of this model is a set of $\langle S, P, O \rangle$ triplets per frame, where S , P , and O represent the *subject*, *predicate*, and *object*, respectively. We keep the $\langle S, O \rangle$ pairs as relation proposals and discard the original predicate semantics, as the relation predicates of the model trained on VG200 are limited and fixed; instead we let our reasoning model learn implicit relation semantics during our end-to-end training. In our trained relation model, N_r is set to 100. Since not all objects are included in the N_r relation proposals, we prune the graph nodes that are not part of the selected proposals. We then feed the $\langle S, O \rangle$ pairs to the next ROI recrop step.

Union Box ROI Recrop: For the detected $\langle S, O \rangle$ pairs, we regard the union box of the bounding boxes for S and O as the predicate region of interest. Next, we apply the *ROI-align* operator [43] on the last layer of the backbone network using this union box and make the resultant feature an extra node in the scene graph; more specifically, if R_e denotes the new recrop node feature, then our updated graph between S and O has a new structure denoted $S - R_e - O$, and the new edges $S - R_e$ and $R_e - O$ are implicitly learned (see the Semantic Scene Graph Reasoning section below). In contrast to representing the predicate or relation as an edge, representing the predicate as an extra node is advantageous. For example, the union box covers more information than both the subject and object bounding boxes, thereby capturing higher-order interactions between them, while bottom-up and top-down features only capture information within single bounding boxes.

3.2 Intra-Graph Reasoning

Representing videos directly as sequences of scene graphs leads to a complex graph reasoning problem that is likely to be computationally intractable. To avoid this issue, we propose to hierarchically reduce the complexity by embedding these graphs into learned representation spaces. Specifically, we propose an intra-graph reasoning scheme that bifurcates a scene graph into two streams: (i) a *visual scene graph* that generates a representation summarizing the visual cues captured in the graph nodes, and (ii) a *semantic scene graph* that summarizes the graph edges. Formally, let us define a scene graph as $\mathcal{G} = \{(x_i, e_{ij}, x_j) \mid x_i, x_j \in \mathcal{V}, e_{ij} \in \mathcal{E}\}$, where \mathcal{V} denotes the set of nodes consisting of single objects and \mathcal{E} is the set of edges consisting of relations linking two objects. The triplet (x_i, e_{ij}, x_j)

indicates that the subject node x_i and the object node x_j are connected by the directed relation edge e_{ij} . We denote by \mathcal{G}_v and \mathcal{G}_s the visual scene graph and the semantic scene graph respectively: the former is a graph attention network [51] which computes an attention coefficient for each edge and updates node features based on these coefficients; the latter is based on EdgeConv [55], which computes extra edge features based on node features and then updates node features by aggregating linked edge features. Both networks are explained in more details below. We combine these two complementary graph neural networks in a cascade way to conduct intra-graph reasoning.

Visual Scene Graph Reasoning: For M node features $\mathbf{X} = \{\mathbf{x}_1, \mathbf{x}_2, \dots, \mathbf{x}_M\}$ in a scene graph, multi-head self-attention [50] is first performed for each pair of linked nodes. In each head k , for two linked nodes \mathbf{x}_i and \mathbf{x}_j , the attention coefficient α_{ij}^k indicating the importance of node j to node i is calculated by

$$\alpha_{ij}^k = \frac{\exp(\sigma(\Theta_k^T [\mathbf{W}_1^k \mathbf{x}_i \parallel \mathbf{W}_1^k \mathbf{x}_j]))}{\sum_{k \in \mathcal{N}_i} \exp(\sigma(\Theta_k^T [\mathbf{W}_1^k \mathbf{x}_i \parallel \mathbf{W}_1^k \mathbf{x}_k]))}, \quad (2)$$

where \parallel denotes the feature concatenation, σ is a nonlinearity (leaky ReLU), \mathcal{N}_i indicates the neighboring graph nodes of object i , $\mathbf{W}_1^k \in \mathbb{R}^{d_h \times d_{in}}$ is a (learned) weight matrix transforming the original features to a shared latent space, and $\Theta_k \in \mathbb{R}^{2d_h}$ is the (learned) attention weight vector. Using the attention weights α^k and a set of learned weight matrices $\mathbf{W}_2^k \in \mathbb{R}^{d_h/K \times d_{in}}$, we update the node features as:

$$\mathbf{x}'_i = \parallel_{k=1}^K \sigma \left(\sum_{j \in \mathcal{N}_i} \alpha_{ij}^k \mathbf{W}_2^k \mathbf{x}_j \right). \quad (3)$$

Outputs of the K heads are concatenated to produce $\mathbf{x}'_i \in \mathbb{R}^{d_h}$, which is used as input to the semantic graph network.

Semantic Scene Graph Reasoning: This sub-module captures higher-order semantics between nodes in the scene graph. To this end, EdgeConv [55], which is a multi-layer fully-connected network h_{Λ} , is employed to generate edge features \mathbf{e}_{ij} from its two connected node features $(\mathbf{x}'_i, \mathbf{x}'_j)$:

$$\mathbf{e}_{ij} = h_{\Lambda}(\mathbf{x}'_i, \mathbf{x}'_j), \quad (4)$$

where $h_{\Lambda} : \mathbb{R}^{d_h} \times \mathbb{R}^{d_h} \rightarrow \mathbb{R}^{d_h}$ is a nonlinear transformation with learnable parameters Λ . We then produce the output node features \mathbf{x}_i^* by aggregating features from the edges that are directed to the object node i , i.e.,

$$\mathbf{x}_i^* = \max_{j:(j,i) \in \mathcal{E}_i} \mathbf{e}_{ji}, \quad (5)$$

where \mathcal{E}_i denotes the set of edges directed to node i . All object features inside the scene graph are updated by the above intra-graph feature aggregations.

Memory Generation with Graph Pooling: After conducting intra-graph reasoning to obtain higher-level features for each node, we want to pool the updated graph into a memory for further temporal aggregation. Since different frame-level scene graphs have different numbers of nodes and edges, we adopt

graph average pooling (GAP) and graph max pooling (GMP) [32] to generate two graph memories and concatenate them as the final graph memory V^* :

$$V^* = \text{GAP}(\mathbf{X}^*, \mathcal{E}) \parallel \text{GMP}(\mathbf{X}^*, \mathcal{E}), \quad (6)$$

where \mathcal{E} denotes the connection structure of the scene graph, and \mathbf{X}^* denotes the M final node features $\{\mathbf{x}_1^*, \mathbf{x}_2^*, \dots, \mathbf{x}_M^*\}$ from (5).

3.3 Inter-Graph Information Aggregation

So far, we have generated graph memories by intra-graph reasoning and graph pooling, as described above. In addition to these spatial graph manipulations, there is a temporal continuity of visual cues from the video frames that need to be captured in the visual representation. Towards aggregation of this temporal information, we propose an inter-graph aggregation scheme that operates on the graph embeddings. Specifically, for a sequence of scene graph memories $\langle v_1^*, v_2^*, \dots, v_L^* \rangle$ of length L produced using (6) on a sequence of L frames, we use temporal sliding windows of size T to update the graph memory of the center frame in each window by aggregating the graph memories of its neighboring frames in that window, both in the past and the future. Let $f \in \mathbb{R}^{2d_h \times T}$ denote a matrix of graph embeddings within this window of length T , then we perform window-level summerization over all frame memories within f as:

$$\alpha = \text{softmax}(P_\alpha^T \tanh(\mathbf{W}_t f)), \quad (7)$$

where $\mathbf{W}_t \in \mathbb{R}^{2d_h \times 2d_h}$ is a learned weight matrix, $P_\alpha \in \mathbb{R}^{2d_h}$ a weight vector, and $\alpha \in \mathbb{R}^T$ denote the attention weights. We then use α to update the memory of the center frame v_c by aggregating information across this window, as:

$$v_c = \alpha f^T. \quad (8)$$

Repeating this step for all sliding windows, we get the final graph memory sequence $V = \{v_1, v_2, \dots, v_L\}$ aggregating both spatial and temporal information.

3.4 Semantics-Controlled Transformer Reasoning

The above modules encode a video into a sequence of graph memories via reasoning on visual and semantic scene graphs. Besides such a video encoder, we still need to encode text information available with the AVSD task and learn a dialog model that can generate the answer. Following prior works [2,25], we propose to generate the answer autoregressively. That is, we formulate this sentence generation problem as that of predicting the next word from the vocabulary based on source sequences including query Q_l , caption C , the dialog history $H = \langle (Q_1, A_1), \dots, (Q_{l-1}, A_{l-1}) \rangle$, and the partially generated answer so far, denoted A_l^{in} (see Fig. 2 and Fig. 3(a)). This sub-answer A_l^{in} forms the semantics that control the attention on the various modalities to generate the next word. As shown in Fig. 3(a), our semantics-controlled transformer module consists of a graph encoder, a text encoder, and a multimodal decoder. It takes in source

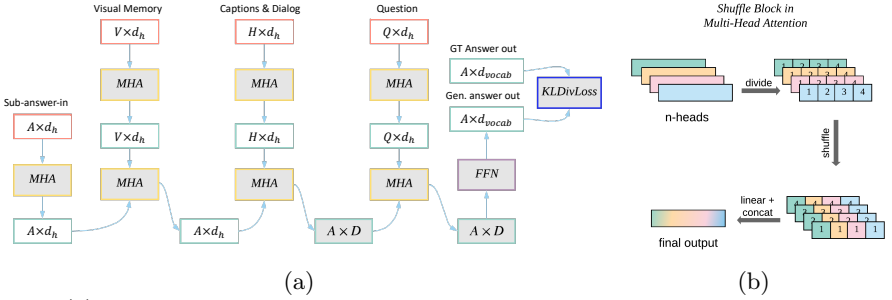


Fig. 3. (a) depicts our semantics-controlled transformer, the dimensionality of the multimodal embeddings, and the attention flow. MHA and FFN denote multi-head attention and feed-forward networks, respectively, as in [50]. The acronyms A, V, H, and Q stand for the embedding dimensions of the answers, visual memory, caption/dialog history (which are concatenated), and the question, respectively. (b) illustrates our multi-head shuffled transformer, where we shuffle the output of each head before passing it on to the FFN module.

sequences and outputs the probability distribution of being the next token for all tokens in the vocabulary. We detail the steps in this module next.

Encoder: Following Vaswani et al. [50], we first embed all text sources (H, C, Q_l, A_i^{in}) using token and positional embeddings as to generate multimodal feature matrices e_h, e_c, e_q, e_a , each of the same feature dimensionality d_h as shown in Fig. 3(a). We also use a single-layer fully-connected network to transfer the $2d_h$ -dimensional visual memories in V to d_h -dimensional features e_v that match the dimension of the text sources. Next, the input sub-answer (generated so far) e_a is encoded with a transformer consisting of multi-head self-attention to obtain encoded hidden representations h_{enc}^a :

$$h_{enc}^a = \text{FFN}^a(\text{Attention}(\mathbf{W}_q^a e_a, \mathbf{W}_k^a e_a, \mathbf{W}_v^a e_a)), \quad (9)$$

where $\mathbf{W}_q^a, \mathbf{W}_k^a, \mathbf{W}_v^a$ are weight matrices for query, key, and value respectively [50], FFN^a is a feed-forward module consisting of two fully-connected layers with ReLU in between, and the Attention function is defined as in [50]:

$$\text{Attention}(Q, K, V) = \text{softmax}\left(\frac{QK^T}{\sqrt{d_h}}\right)V, \quad (10)$$

where the scaling factor $\sqrt{d_h}$ maintains the order of magnitude in features. After encoding the input sub-answer, we conduct co-attention in turn for each of the other text and visual embeddings e_j , where $j \in \{v, c, h, q\}$, with a similar Transformer structure. The encoding h_{enc}^j for a given embedding type e_j is obtained by using the encoding $h_{enc}^{j'}$ for the previous embedding type $e_{j'}$ as query:

$$h_{enc}^j = \text{FFN}^j(\text{Attention}(\mathbf{W}_q^j h_{enc}^{j'}, \mathbf{W}_k^j e_j, \mathbf{W}_v^j e_j)). \quad (11)$$

In our implementation, the embeddings for history and caption are concatenated as $e_{c+h} = e_c || e_h$. Processing occurs in the following order: starting from h_{enc}^a , we compute h_{enc}^v , then h_{enc}^{c+h} , and finally h_{enc}^q . Finally, we get a feature vector h_{enc}^*

that fuses all the information from the text and visual sources by concatenating these multimodal features.

Multi-head Shuffled Transformer: In this paper, we also propose to utilize head shuffling to further improve the performance of the Transformer structure as shown in Fig. 3(b). In the original Transformer [50], the feature vectors of all heads are concatenated before being fed into the last fully-connected layer. Thus, there is no interaction between those heads from the start to the end. To overcome this drawback, we propose to shuffle these head vectors before feeding them into fully-connected layers and concatenate them in a late fusion style. This scheme is similar to ShuffleNet [69], with the key difference that here we conduct shuffling between different heads within the multi-head attention, while in ShuffleNet the shuffling is across channels. Our empirical results show that our shuffling operation results in better generalization of the model.

Decoder: With the final encoded feature h_{enc}^* , we use a feed-forward network with softmax to predict the next token probability distribution P over all tokens in the vocabulary \mathcal{V} :

$$P = \text{softmax}(\text{FFN}(h_{\text{enc}}^*)). \quad (12)$$

In the testing stage, we conduct beam search with b beams to generate an answer sentence. In each step, we select b tokens with the top- b highest confidence scores. The answer generation is stopped either when token $\langle eos \rangle$ is produced or when reaching the maximum number of tokens.

Loss Function: Let \mathcal{P} denote the collection of all next-token probability distributions P_j within a batch, where $j = 1, \dots, N$ indexes a token in the batch (each batch element corresponds to a single word from a response to be predicted), and \mathcal{G} the collection of distributions G_j of ground truth answer tokens. We apply label smoothing [38] to account for the sparsity of the token distributions, leading to $\tilde{\mathcal{G}}$. We use the cross-entropy loss between the predicted and the smoothed ground truth token distributions to train our STSGR model end-to-end:

$$\mathcal{L} = \text{CE}(\mathcal{P}|\tilde{\mathcal{G}}) = -\frac{1}{N} \sum_{j=1}^N \sum_{u \in \mathcal{V}} \tilde{G}_j(u) \ln P_j(u). \quad (13)$$

4 Experiments

We present experiments on two versions of the AVSD dataset. We also provide ablation studies and compare our approach to recent state-of-the-art methods.

Dataset: The audio-visual scene-aware dialog (AVSD) dataset [1] emulates a real-world human-human natural conversation scenario about an audio-visual clip. See [1] for details on this task and the dataset. The AVSD official dataset for natural language generation contains 7,659, 1,787, 1,710, and 1,710 dialogs for training, validation, DSTC-7 testing, and DSTC-8 testing, respectively.

Evaluation: The official objective metrics for natural language generation evaluation are those of the MSCOCO evaluation tool, which includes 4 word-overlap-based metrics such as BLUE 1 to 4, METEOR, ROUGE-L, and CIDEr [8]. In

this paper, we also report human evaluation for the AVSD@DSTC8 test split (provided to us by the organizers of the official DSTC-8 challenge.²). Compared with objective metrics, human evaluation is more robust and allows better recognition of good, semantically correct, and natural generated answers, even though they may not match exactly with the ground truth. Specifically, human ratings for each system response use a 5 point scale: 5 for Very good, 4 for Good, 3 for Acceptable, 2 for Poor, 1 for Very poor. When evaluating, human raters consider not only correctness of the answers but also naturalness, informativeness, and appropriateness of the response according to the given context.

Data Processing: We follow [31] to perform text preprocessing which include lowercasing, tokenization, and building a vocabulary by only selecting tokens that happen at least five times. Thus, we use a vocabulary with 3,254 words.

Feature Extraction: Motivated by Anderson et al. [2], we train a new detector on Visual Genome with 1601 classes and 401 attributes. We also incorporate a “background” label and a “no-attribute” label. We use ResNext-101 as neural backbone with multiscale feature pyramid network. Further, we use fine-grained ROI-alignment instead of ROI-pooling for better feature representation, specifically, ROI-alignment uses bilinear interpolation while ROI-pooling uses nearest neighbours to crop original feature map; the latter may introduce quantization errors which are not differentiable. We extract the 1024-D features for the first 36 highest scoring regions, their class labels, and attributes. After extracting the region features, we apply a Visual-Genome-trained relationship detector to find visually-related regions. We calculate the minimal bounding box which can cover two visually-related regions and perform an ROI-alignment to get a compact representation for relationship regions.

Model Training: We set our Transformer hyperparameters following [50]. The feature dimension is 512, while the inner-layer dimension of the feed-forward network is set to 2048. For multi-head attention, we maintain $h = 8$ parallel attention heads and apply shuffling to boost performance. For the semantic labels, we build a 300-D embedding layer for the 1651 words in the vocabulary (which is available with the dataset), and initialize the embeddings using GloVe word vectors [42]. For semantic labels consisting of more than one word, we use the average word embedding as the label embedding. Our model is trained on one Nvidia Titan XP GPU with Adam optimizer [29] with $\beta_1 = 0.9$, $\beta_2 = 0.98$. The batch size is set to 16 and we adopt the warm-up strategy suggested in [50] for learning rate adjustment with 10000 warm-up steps.

Baselines: We consider the following four baselines from recent papers for performance comparison with our proposed STSGR model: (i) *Baseline* [23] provided with the DSTC challenge, (ii) *Multimodal Attention* [23], that uses attention over concatenated features, (iii) *Simple* [45] that computes VGG features on frames, followed by factor-graph attention on the modalities, and (iv) *MTN* [31] that applies self-attention and co-attention to aggregate multimodal information.

² <https://sites.google.com/dstc.community/dstc8/home>

Ablation Study: To understand the importance of each component in our model, Table 1 details an ablation study. We analyze several key components: (i) shuffling in the Transformer structure, (ii) visual and semantic graph, (iii) ROI Recrop on the union bounding boxes, and (iv) temporal aggregation. From the table, we see that Graph Attention Network (GAT), which is used to produce the visual scene graph, is important to aggregate information from neighboring nodes (e.g., improving CIDEr from 1.125 to 1.265), while EdgeConv, used in the semantic graph, offers some improvement (e.g., CIDEr from 1.244 to 1.265). Moreover, the use of shuffling in the multi-head Transformer structure boosts the performance significantly (from 1.208 to 1.265 for CIDEr). We can also conclude that union bounding boxes, semantic labels, and inter-graph reasoning contribute to stabilize the generation performance. Overall, by adopting all these key components, the full model outperforms all the ablations.

Method	BLUE-1	BLUE-2	BLUE-3	BLUE-4	METEOR	ROUGE	CIDEr
Full model	0.362	0.249	0.179	0.133	0.165	0.361	1.265
w/o shuffle	0.354	0.242	0.172	0.127	0.161	0.354	1.208
w/o GAT	0.337	0.227	0.161	0.118	0.160	0.347	1.125
w/o EdgeConv	0.358	0.244	0.176	0.131	0.162	0.356	1.244
w/o union box feature	0.354	0.239	0.170	0.124	0.163	0.352	1.175
w/o semantic graph	0.356	0.241	0.172	0.127	0.160	0.356	1.203
w/o temporal	0.355	0.240	0.170	0.125	0.164	0.357	1.212

Table 1. Ablation study on STSGR using AVSD@DSTC7 dataset.

Comparisons to State-of-the-Art Methods: In Table 2, we compare STSGR against the baseline methods listed above on various language quality metrics based on ground truth answers. We also provide the human evaluation rating on the AVSD@DSTC8 test split. As is clear from the results, our approach achieves state-of-the-art performance against all the baselines. Table 2 shows that our STSGR improves the human rating from 3.064 in [44] to 3.433, a 12% relative improvement. We also attempted to include audio into our framework using the VGGish features available with the AVSD dataset. However, we found that these features did not improve the performance, suggesting perhaps we need more powerful audio embeddings, research into which is beyond our current focus.

AVSD@DSTC7						
Method	Feature	BLUE-4	METEOR	ROUGE	CIDEr	Human
Baseline [23]	R+F+A	0.075	0.110	0.275	0.701	NA
Multimodal Attention [23]	R+F+A	0.078	0.113	0.277	0.727	NA
Simple [44]	R+F	0.091	0.125	0.307	0.883	NA
MTN [31]	F+A	0.128	0.162	0.355	1.249	NA
STSGR (Ours)	scene graph	0.133	0.165	0.361	1.265	NA
AVSD@DSTC8						
Baseline [23]	R+F	0.289	0.21	0.48	0.651	2.885
Simple [44]	R+F	0.311	0.224	0.502	0.766	3.064
STSGR (Ours)	scene graph	0.357	0.267	0.553	1.004	3.433

Table 2. Comparisons of STSGR against state of the art AVSD test split on DSTC7 and DSTC8 challenges. Acronyms: R=I3D RGB, F=I3D flow, A=VGGish.

Method	Feature	B4	M	R	C
Simple	i3d	0.091	0.125	0.307	0.883
Simple	VGG	0.095	0.126	0.309	0.919
MTN	N/A	0.114	0.147	0.332	1.106
MTN	i3d	0.118	0.160	0.348	1.151
STSGR (Ours)	N/A	0.121	0.152	0.350	1.186
STSGR (Ours)	i3d	0.122	0.152	0.353	1.223
STSGR (Ours)	Scene Graphs	0.133	0.165	0.361	1.265

Table 3. Comparison of visual representations against STSGR on AVSD@DSTC7.

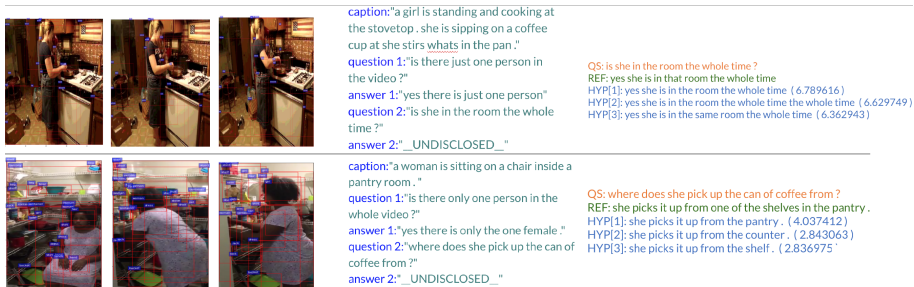


Fig. 4. Qualitative results from our STSGR model. Left: the input video frames, Middle: the caption and the dialog history, Right: the question, the ground truth answer, and top-3 generated answers. More results in the supplementary materials.

Qualitative Results and Discussion: In Fig. 4, we provide two qualitative results from our STSGR model. For the first case, our model consistently detects the woman in the frames and finds that she maintains many connections with other objects inside the scene throughout the whole video, thus our model makes the correct answer with high confidence. To understand how the model works, we attempted to remove the woman node from the last one third of all input frames, to see that now the model outputs no she leaves the room in the end. When removing this node from one or two frames, output remains yes she is in the room the whole time, suggesting that our inter-graph reasoning is indeed learning persistence of graph nodes across time. For the second case, STSGR captures the semantics of the pantry room and help to generate a correct response “she picks it up from the pantry”, although the second and third responses refine this answer with more specific (correct) details.

In general, we find that STSGR can answer spatial and temporal questions very well. This is quantitatively evidenced by observing that while both STSGR and MTN [31] use similar backends, they differ in the input representations (I3D in [31] vs. scene graphs in ours), and our model outperforms MTN by a significant baseline (1.265 vs 1.249 on CIDEr), substantiating the importance of our STSGR representation. In Table 3, we further compare STSGR with other visual representations on different methods, establishing the benefits.

5 Conclusions

We proposed a spatio-temporal scene graph representation for solving the multimodal question answering problem on the AVSD task. Our representation captures the fine-grained details of local image content, alongside its spatio-temporal relationships, using a hierarchical reasoning setup and a multimodal co-attention scheme effectuated using a shuffled transformer framework. Experiments demonstrating state-of-the-art results on two tracks of the popular AVSD challenge dataset show that our proposed representation is very effective in characterizing the visual content.

A STSGR and Audio Features

The AVSD dataset provides pre-computed audio features, encoded using the VGGish model. These are 128D features, one for every video clip, extracted from a VGG-like neural network model trained on mel-frequency spectrum of the audio associated with the video clips. In Table 4, we study the influence of these VGGish features on STSGR and baseline methods (Baseline [23] MTN [68]). Both Baseline and MTN use holistic representations of the video using the I3D features. While the improvement of Baseline with the addition of VGGish features is very marginal, the transformer networks used in MTN seems to make a better use of these features. However, with STSGR, VGGish does not offer any significant advantages. This is perhaps because, our STSGR uses very fine-grained features from the frames, however the VGGish features are not directly correlated with these frame-level STSGR representations (they are computed for the video as a whole), and thus do not provide any useful details over what is already provided by STSGR. It may also suggest that perhaps we might need a better audio-visual architecture, which is outside the scope of this paper.

Method	BLUE-1	BLUE-2	BLUE-3	BLUE-4	METEOR	ROUGE	CIDEr
Baseline [23]	0.269	0.172	0.117	0.083	0.117	0.29	0.771
Baseline + VGGish	0.273	0.173	0.118	0.084	0.116	0.292	0.775
MTN	0.343	0.229	0.161	0.118	0.160	0.348	1.151
MTN + VGGish	0.357	0.241	0.173	0.128	0.162	0.355	1.249
STSGR	0.362	0.249	0.179	0.133	0.165	0.361	1.265
STSGR+VGGish	0.355	0.241	0.172	0.126	0.159	0.352	1.225

Table 4. Influence of Audio features on STSGR performance.

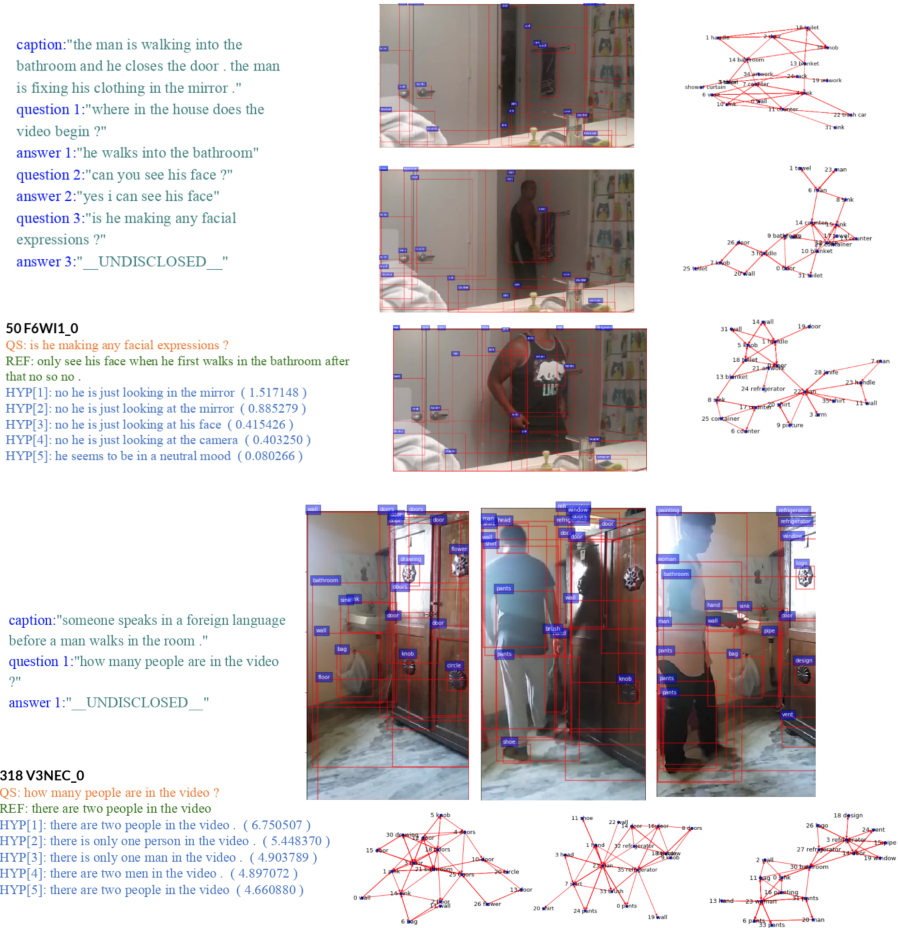


Fig. 5. For the first example, our model perhaps used the caption to come to the conclusion that the man is not looking at the mirror. For the second example, our model perhaps used the scene graphs to reason about the number of people in the room. For example, it appears that there are in fact two people in the video, however they occur individually in the frames. The last scene graph seems to detect a man and a woman in the frame, which is a false positive. Thus, the model seems to confuse between a single person or two people, as is shown in the answers produced by the model. We believe this is a legitimate confusion, and is perhaps the result of an inexact object detection/scene graph generation.

References

1. Alamri, H., Cartillier, V., Das, A., Wang, J., Cherian, A., Essa, I., Batra, D., Marks, T.K., Hori, C., Anderson, P., et al.: Audio visual scene-aware dialog. In: Proc. IEEE Conference on Computer Vision and Pattern Recognition (CVPR). pp. 7558–7567 (2019)
2. Anderson, P., He, X., Buehler, C., Teney, D., Johnson, M., Gould, S., Zhang, L.: Bottom-up and top-down attention for image captioning and visual question answering. In: Proc. IEEE Conference on Computer Vision and Pattern Recognition (CVPR) (2018)
3. Antol, S., Agrawal, A., Lu, J., Mitchell, M., Batra, D., Lawrence Zitnick, C., Parikh, D.: Vqa: Visual question answering. In: Proc. IEEE International Conference on Computer Vision (ICCV). pp. 2425–2433 (2015)
4. Ben-Younes, H., Cadene, R., Thome, N., Cord, M.: Block: Bilinear superdiagonal fusion for visual question answering and visual relationship detection. In: AAAI (2019)
5. Carreira, J., Zisserman, A.: Quo vadis, action recognition? a new model and the kinetics dataset. In: Proc. IEEE Conference on Computer Vision and Pattern Recognition (CVPR). pp. 6299–6308 (2017)
6. Chen, K., Wang, J., Pang, J., Cao, Y., Xiong, Y., Li, X., Sun, S., Feng, W., Liu, Z., Xu, J., Zhang, Z., Cheng, D., Zhu, C., Cheng, T., Zhao, Q., Li, B., Lu, X., Zhu, R., Wu, Y., Dai, J., Wang, J., Shi, J., Ouyang, W., Loy, C.C., Lin, D.: MMDetection: Open mmlab detection toolbox and benchmark. arXiv preprint arXiv:1906.07155 (2019)
7. Chen, V.S., Varma, P., Krishna, R., Bernstein, M., Re, C., Fei-Fei, L.: Scene graph prediction with limited labels. In: Proc. IEEE Conference on Computer Vision and Pattern Recognition (CVPR) (2019)
8. Chen, X., Fang, H., Lin, T.Y., Vedantam, R., Gupta, S., Dollár, P., Zitnick, C.L.: Microsoft COCO captions: Data collection and evaluation server. arXiv preprint arXiv:1504.00325 (2015)
9. Das, A., Kottur, S., Gupta, K., Singh, A., Yadav, D., Moura, J.M., Parikh, D., Batra, D.: Visual dialog. In: Proc. IEEE Conference on Computer Vision and Pattern Recognition (CVPR) (2017)
10. De Vries, H., Strub, F., Chandar, S., Pietquin, O., Larochelle, H., Courville, A.: Guesswhat?! visual object discovery through multi-modal dialogue. In: Proc. IEEE Conference on Computer Vision and Pattern Recognition (CVPR) (2017)
11. De Vries, H., Strub, F., Mary, J., Larochelle, H., Pietquin, O., Courville, A.C.: Modulating early visual processing by language. In: Proc. Advances in Neural Information Processing Systems (IPS). pp. 6594–6604 (2017)
12. Deruyttere, T., Vandenhende, S., Grujicic, D., Van Gool, L., Moens, M.F.: Talk2car: Taking control of your self-driving car. arXiv preprint arXiv:1909.10838 (2019)
13. Dornadula, A., Narcomey, A., Krishna, R., Bernstein, M., Li, F.F.: Visual relationships as functions: Enabling few-shot scene graph prediction. In: ICCV Workshops (2019)
14. Drossos, K., Lipping, S., Virtanen, T.: Clotho: An audio captioning dataset. arXiv preprint arXiv:1910.09387 (2019)
15. Ferrari, V., Zisserman, A.: Learning visual attributes. In: Proc. Advances in Neural Information Processing Systems (IPS) (2008)

16. Fukui, A., Park, D.H., Yang, D., Rohrbach, A., Darrell, T., Rohrbach, M.: Multi-modal compact bilinear pooling for visual question answering and visual grounding. arXiv preprint arXiv:1606.01847 (2016)
17. Gan, Z., Cheng, Y., Kholy, A.E., Li, L., Liu, J., Gao, J.: Multi-step reasoning via recurrent dual attention for visual dialog. arXiv preprint arXiv:1902.00579 (2019)
18. Gao, P., Jiang, Z., You, H., Lu, P., Hoi, S.C.H., Wang, X., Li, H.: Dynamic fusion with intra- and inter-modality attention flow for visual question answering. In: Proc. IEEE Conference on Computer Vision and Pattern Recognition (CVPR) (Jun 2019)
19. Gao, P., Li, H., Li, S., Lu, P., Li, Y., Hoi, S.C., Wang, X.: Question-guided hybrid convolution for visual question answering. In: Proc. European Conference on Computer Vision (ECCV). pp. 469–485 (2018)
20. Geman, D., Geman, S., Hallonquist, N., Younes, L.: Visual turing test for computer vision systems. *Proceedings of the National Academy of Sciences* **112**(12), 3618–3623 (2015)
21. Ghosh, S., Burachas, G., Ray, A., Ziskind, A.: Generating natural language explanations for visual question answering using scene graphs and visual attention. arXiv preprint arXiv:1902.05715 (2019)
22. Girdhar, R., Carreira, J., Doersch, C., Zisserman, A.: Video action transformer network. In: Proc. IEEE Conference on Computer Vision and Pattern Recognition (CVPR) (2019)
23. Hori, C., Alamri, H., Wang, J., Wichern, G., Hori, T., Cherian, A., Marks, T.K., Cartillier, V., Lopes, R.G., Das, A., et al.: End-to-end audio visual scene-aware dialog using multimodal attention-based video features. In: Proc. IEEE International Conference on Acoustics, Speech and Signal Processing (ICASSP). pp. 2352–2356 (May 2019)
24. Hori, C., Hori, T., Lee, T.Y., Zhang, Z., Harsham, B., Hershey, J.R., Marks, T.K., Sumi, K.: Attention-based multimodal fusion for video description. In: Proc. IEEE International Conference on Computer Vision (ICCV). pp. 4193–4202 (2017)
25. Hori, C., Hori, T., Wichern, G., Wang, J., Lee, T.y., Cherian, A., Marks, T.K.: Multimodal attention for fusion of audio and spatiotemporal features for video description. In: Proc. CVPR Workshops. pp. 2528–2531 (2018)
26. Jain, A., Zamir, A.R., Savarese, S., Saxena, A.: Structural-rnn: Deep learning on spatio-temporal graphs. In: Proc. IEEE Conference on Computer Vision and Pattern Recognition (CVPR) (2016)
27. Jang, Y., Song, Y., Yu, Y., Kim, Y., Kim, G.: TGIF-QA: Toward spatio-temporal reasoning in visual question answering. In: Proc. IEEE Conference on Computer Vision and Pattern Recognition (CVPR) (2017)
28. Johnson, J., Krishna, R., Stark, M., Li, L.J., Shamma, D., Bernstein, M., Fei-Fei, L.: Image retrieval using scene graphs. In: Proc. IEEE Conference on Computer Vision and Pattern Recognition (CVPR) (2015)
29. Kingma, D.P., Ba, J.: Adam: A method for stochastic optimization. *Proc. International Conference on Learning Representations (ICLR)* (2015)
30. Krishna, R., Zhu, Y., Groth, O., Johnson, J., Hata, K., Kravitz, J., Chen, S., Kalantidis, Y., Li, L.J., Shamma, D.A., et al.: Visual Genome: Connecting language and vision using crowdsourced dense image annotations. *International Journal of Computer Vision* **123**(1), 32–73 (2017)
31. Le, H., Sahoo, D., Chen, N.F., Hoi, S.C.: Multimodal transformer networks for end-to-end video-grounded dialogue systems. arXiv preprint arXiv:1907.01166 (2019)
32. Lee, J., Lee, I., Kang, J.: Self-attention graph pooling (2019)

33. Lei, J., Yu, L., Bansal, M., Berg, T.L.: TVQA: Localized, compositional video question answering. arXiv preprint arXiv:1809.01696 (2018)
34. Li, G., Zhu, L., Liu, P., Yang, Y.: Entangled transformer for image captioning. In: Proc. IEEE International Conference on Computer Vision (ICCV) (Oct 2019)
35. Li, L., Gan, Z., Cheng, Y., Liu, J.: Relation-aware graph attention network for visual question answering. arXiv preprint arXiv:1903.12314 (2019)
36. Li, X., Jiang, S.: Know more say less: Image captioning based on scene graphs. IEEE Transactions on Multimedia **21**(8), 2117–2130 (2019)
37. Lu, C., Krishna, R., Bernstein, M., Fei-Fei, L.: Visual relationship detection with language priors. In: European Conference on Computer Vision (2016)
38. Müller, R., Kornblith, S., Hinton, G.E.: When does label smoothing help? In: Proc. Advances in Neural Information Processing Systems (NeurIPS) (2019)
39. Newell, A., Deng, J.: Pixels to graphs by associative embedding. In: Proc. Advances in Neural Information Processing Systems (IPS) (2017)
40. Noh, H., Hongsuck Seo, P., Han, B.: Image question answering using convolutional neural network with dynamic parameter prediction. In: Proc. IEEE Conference on Computer Vision and Pattern Recognition (CVPR). pp. 30–38 (2016)
41. Norcliffe-Brown, W., Vafeias, S., Parisot, S.: Learning conditioned graph structures for interpretable visual question answering. In: Proc. Advances in Neural Information Processing Systems (NeurIPS) (2018)
42. Pennington, J., Socher, R., Manning, C.: GloVe: Global vectors for word representation. In: Proc. Conference on Empirical Methods in Natural Language Processing (EMNLP) (2014)
43. Ren, S., He, K., Girshick, R., Sun, J.: Faster R-CNN: Towards real-time object detection with region proposal networks. In: Proc. Advances in Neural Information Processing Systems (IPS) (2015)
44. Schwartz, I., Schwing, A.G., Hazan, T.: A simple baseline for audio-visual scene-aware dialog. In: Proc. IEEE Conference on Computer Vision and Pattern Recognition (CVPR). pp. 12548–12558 (2019)
45. Schwartz, I., Yu, S., Hazan, T., Schwing, A.G.: Factor graph attention. In: Proc. IEEE Conference on Computer Vision and Pattern Recognition (CVPR) (2019)
46. Teney, D., Liu, L., van Den Hengel, A.: Graph-structured representations for visual question answering. In: Proc. IEEE Conference on Computer Vision and Pattern Recognition (CVPR) (2017)
47. Thomason, J., Padmakumar, A., Sinapov, J., Walker, N., Jiang, Y., Yedidsion, H., Hart, J., Stone, P., Mooney, R.J.: Improving grounded natural language understanding through human-robot dialog. In: ICRA (2019)
48. Tran, D., Bourdev, L., Fergus, R., Torresani, L., Paluri, M.: Learning spatiotemporal features with 3d convolutional networks. In: Proc. IEEE International Conference on Computer Vision (ICCV). pp. 4489–4497 (2015)
49. Tsai, Y.H.H., Divvala, S., Morency, L.P., Salakhutdinov, R., Farhadi, A.: Video relationship reasoning using gated spatio-temporal energy graph. In: Proc. IEEE Conference on Computer Vision and Pattern Recognition (CVPR) (2019)
50. Vaswani, A., Shazeer, N., Parmar, N., Uszkoreit, J., Jones, L., Gomez, A.N., Kaiser, L., Polosukhin, I.: Attention is all you need. In: Proc. Advances in Neural Information Processing Systems (IPS). pp. 5998–6008 (2017)
51. Veličković, P., Cucurull, G., Casanova, A., Romero, A., Lio, P., Bengio, Y.: Graph attention networks. arXiv preprint arXiv:1710.10903 (2017)
52. Venugopalan, S., Rohrbach, M., Donahue, J., Mooney, R., Darrell, T., Saenko, K.: Sequence to sequence-video to text. In: Proc. IEEE International Conference on Computer Vision (ICCV) (2015)

53. Wang, X., Girshick, R., Gupta, A., He, K.: Non-local neural networks. In: Proc. IEEE Conference on Computer Vision and Pattern Recognition (CVPR) (2018)
54. Wang, X., Gupta, A.: Videos as space-time region graphs. In: Proc. European Conference on Computer Vision (ECCV) (2018)
55. Wang, Y., Sun, Y., Liu, Z., Sarma, S.E., Bronstein, M.M., Solomon, J.M.: Dynamic graph cnn for learning on point clouds. *ACM Transactions on Graphics (TOG)* **38**(5), 146 (2019)
56. Wu, Q., Wang, P., Shen, C., Reid, I., Van Den Hengel, A.: Are you talking to me? reasoned visual dialog generation through adversarial learning. In: Proc. IEEE Conference on Computer Vision and Pattern Recognition (CVPR) (2018)
57. Wu, Z., Pan, S., Chen, F., Long, G., Zhang, C., Yu, P.S.: A comprehensive survey on graph neural networks. *arXiv preprint arXiv:1901.00596* (2019)
58. Xu, D., Zhao, Z., Xiao, J., Wu, F., Zhang, H., He, X., Zhuang, Y.: Video question answering via gradually refined attention over appearance and motion. In: Proc. ACM Multimedia (2017)
59. Xu, K., Ba, J., Kiros, R., Cho, K., Courville, A., Salakhudinov, R., Zemel, R., Bengio, Y.: Show, attend and tell: Neural image caption generation with visual attention. In: Proc. International Conference on Machine Learning (ICML). pp. 2048–2057 (Jul 2015)
60. Yang, H., Chaisorn, L., Zhao, Y., Neo, S.Y., Chua, T.S.: VideoQA: question answering on news video. In: ICME (2003)
61. Yang, J., Lu, J., Lee, S., Batra, D., Parikh, D.: Graph R-CNN for scene graph generation. In: Proc. European Conference on Computer Vision (ECCV) (2018)
62. Yang, X., Tang, K., Zhang, H., Cai, J.: Auto-encoding scene graphs for image captioning. In: Proc. IEEE Conference on Computer Vision and Pattern Recognition (CVPR) (2019)
63. Yao, T., Pan, Y., Li, Y., Mei, T.: Exploring visual relationship for image captioning. In: Proc. European Conference on Computer Vision (ECCV) (2018)
64. Yeh, Y.T., Lin, T.C., Cheng, H.H., Deng, Y.H., Su, S.Y., Chen, Y.N.: Reactive multi-stage feature fusion for multimodal dialogue modeling. *arXiv preprint arXiv:1908.05067* (2019)
65. Yu, B., Yin, H., Zhu, Z.: Spatio-temporal graph convolutional networks: A deep learning framework for traffic forecasting. *arXiv preprint arXiv:1709.04875* (2017)
66. Zhang, J., Elhoseiny, M., Cohen, S., Chang, W., Elgammal, A.: Relationship proposal networks. In: Proc. IEEE Conference on Computer Vision and Pattern Recognition (CVPR) (July 2017)
67. Zhang, J., Kalantidis, Y., Rohrbach, M., Paluri, M., Elgammal, A., Elhoseiny, M.: Large-scale visual relationship understanding. In: Proc. AAAI Conference on Artificial Intelligence (2019)
68. Zhang, J., Shih, K., Tao, A., Catanzaro, B., Elgammal, A.: An interpretable model for scene graph generation. In: *NeurIPS Workshops* (2018)
69. Zhang, X., Zhou, X., Lin, M., Sun, J.: Shufflenet: An extremely efficient convolutional neural network for mobile devices. In: Proc. IEEE Conference on Computer Vision and Pattern Recognition (CVPR) (2018)
70. Zhou, J., Cui, G., Zhang, Z., Yang, C., Liu, Z., Wang, L., Li, C., Sun, M.: Graph neural networks: A review of methods and applications. *arXiv preprint arXiv:1812.08434* (2018)
71. Zhu, H., Luo, M., Wang, R., Zheng, A., He, R.: Deep audio-visual learning: A survey. *arXiv preprint arXiv:2001.04758* (2020)